International Journal of Environment and Geoinformatics (IJEGEO) is an international, multidisciplinary, peer reviewed, open access journal.

Discrimination of Iron Deposits Using Feature Oriented Principal Component Selection and Band Ratio Methods: Eastern Taurus / TURKEY

Mamadou TRAORE, Tolga ÇAN, Senem TEKİN

Dear colleagues and friends,

International Symposium on Applied Geoinformatics (ISAG2019) was held in Istanbul on 7-9 November 2019. The symposium is organized with the aim of promoting the advancements to explore the latest scientific and technological developments and opportunities in the field of **Geoinformatics**.

The symposium was jointly organized by the **Department of Geomatics Engineering, Yıldız Technical University, Istanbul, Turkey** and the **Institute of Geodesy and Geoinformatics, University of Latvia, Riga-Latvia.**

Our main aim was to bring researchers to share knowledge and their expertise about state-of-art developments in the field of **Geoinformatics**. We wish to discuss the latest developments, opportunities and challenges that can help the **Geoinformatics** community to solve many real-world challenges. Although this forum is initiated by two countries, Turkey and Latvia, it has a global perspective to promote technologies and advancements that would help us live in a better world.

290 participants and scientists from 27 countries were attended to the ISAG2019. 118 oral and 16 poster presentations were presented by 45 international and 89 Turkish presenters in 29 sessions between 7-9 November 2019.

We are much thankful to our supporting institutions Turkish General Directorate of Mapping, The Embassy of Latvia in Turkey, General Directorate of Geographical Information Systems/Turkey, Fatih Municipality.

The presentation "XXX" was presented at the **ISAG2019** and was proposed by our scientific committee for evaluation in the **International Journal of Environmental and Geoinformatics (IJEGEO).**

The next ISAG symposium will be organized in Riga, Latvia on 16-17 November 2021. I do really hope to see you all in Latvia at the 2nd ISAG Symposium.

On behalf of ISAG-2019 Organization Committee

Conference Chair

Prof. Dr. Bülent Bayram

Research Article

Discrimination of Iron Deposits Using Feature Oriented Principal Component Selection and Band Ratio Methods: Eastern Taurus /Turkey

Mamadou Traore*, iD **Tolga Çan,** iD **Senem Tekin** iD

Department of Geological Engineering, Çukurova University, 01330 Sarıçam, Adana, TR

* Corresponding author: M. Traore
 E-mail: matraba77@gmail.com

Abstract

Kayseri and Adana region of Taurus mountain belt is considered in the second range for iron mineralization in Turkey. The region is characterized by high-grade iron ore deposits under exploitation, development and exploration stage. The objective of this research is to assess the potential of Landsat-8 OLI and Advanced Spaceborne Thermal Emission and Reflection Radiometer (ASTER) data for mapping iron oxide zones hosted by carbonate units in low vegetation cover in Tufanbeyli (Adana) and surrounding region. The methods used in this study for the detection of the iron oxides are Band Ratio (BR) and Feature-Oriented Principal Component Selection (FOPCS). The obtained results have good correlation with 92% confidence intervals in BR method for Ferric iron (2/1), ferric oxide (4/3) and ferrous iron (5/4 +1/2) of Aster and iron oxide (4/2) and ferrous iron (6/5) of the Landsat-8. We note that the results obtained in this study using PC4 of FOPCS depict a good spatial correlation by comparison with the previously mapped iron deposits. The significant lithologic groups Carbonate (limestone) be extracted well from ASTER data however alluvium is mapped well in the Landsat -8 OLI image using Band Ratio Color Composite (BRCC). We conclude that the Landsat-8 OLI and Aster images present good precision for iron ore discrimination in low vegetation lands.

Introduction

The Taurus Belt, situated in southern Turkey, is composed mainly of carbonate rocks, in which Fe, Pb–Zn deposits are widespread. The iron ore such as hematite mineralization is widely observed in the basement and overlying units at the eastern part of Tauride-Anatolide platform which are genetically described as volcano syn-sedimentary and/or exhalative syn-sedimentary type mineralization (Tiringa et al., 2011).

Since decades, iron ore is considered an indispensable tool for the development of society. Rocks containing significant amount of iron can be extracted economically (Tuncel et al., 2017). The iron is usually found in the form of magnetite, hematite, goethite, limonite and/or siderite. Iron ore is the raw material used to make pig iron, which is one of the main raw materials in steel production. Demand for raw materials and resources such as iron is increasingly growing in the world.

Remote sensing techniques are increasingly playing an important role in geosciences for mineral exploration and of lithological discrimination (Sabin,1999; Rowan and Mars 2006; Rajendran 2011; Gazioğlu et al., 2014; Avşar et al., 2016; , İncekara et al., 2017; Shirazi et al., 2018; Zoheir et al., 2019). Based on remote sensing data such as Landsat TM, ETM+ and Aster have great potentials in geological interpretations. Remote sensing

is a cost-effective, less time consuming and efficient method for collecting information from poorly accessible remote areas like mountainous or rugged terrains seen in arid and semi-arid regions (Gad and Kusky 2007, Amara et al., 2019).

Several authors have used data from Landsat TM, ETM+ (Sabin, 1999; Abrams et al., 1988) and ASTER (Gad and Kusky, 2007; Safari et al., 2018; Pour et al., 2019; Küçük Matçı and Avdan, 2019) for the exploration of mineral resources and mapping of geological formations in the arid and semi-arid zones. Many studies have proved the potential of remote sensing in the mapping of iron ore using Landsat (Abrams et al., 1983; Sabins, 1997, Ducart et al., 2016) and ASTER (Rajendran, 2011; Huang et al., 2018; Sengupta et al., 2019).

Nine hundred iron deposits were identified in Turkey, of which 496 were studied in the detail by Ünlü et al., (2019). The most economic iron reserves identified in Turkey are located in Sivas-Malatya, Kayseri-Adana, Balıkesir - Kütahya, and Kırşehir–Yozgat regions. In between Kayseri-Adana region is in second range after Sivas - Malatya (Ünlü et al., 2019). The northern Adana, around Tufanbeyli and its vicinity, is characterized by diversity of geological formations (Fig.1). Very little research has been carried out in the area using remote sensing technics. The Zn-Cu-Pb and Fe mineralizations in relation to the main geological settings are determined by MTA (Ünlü et al., 2019).
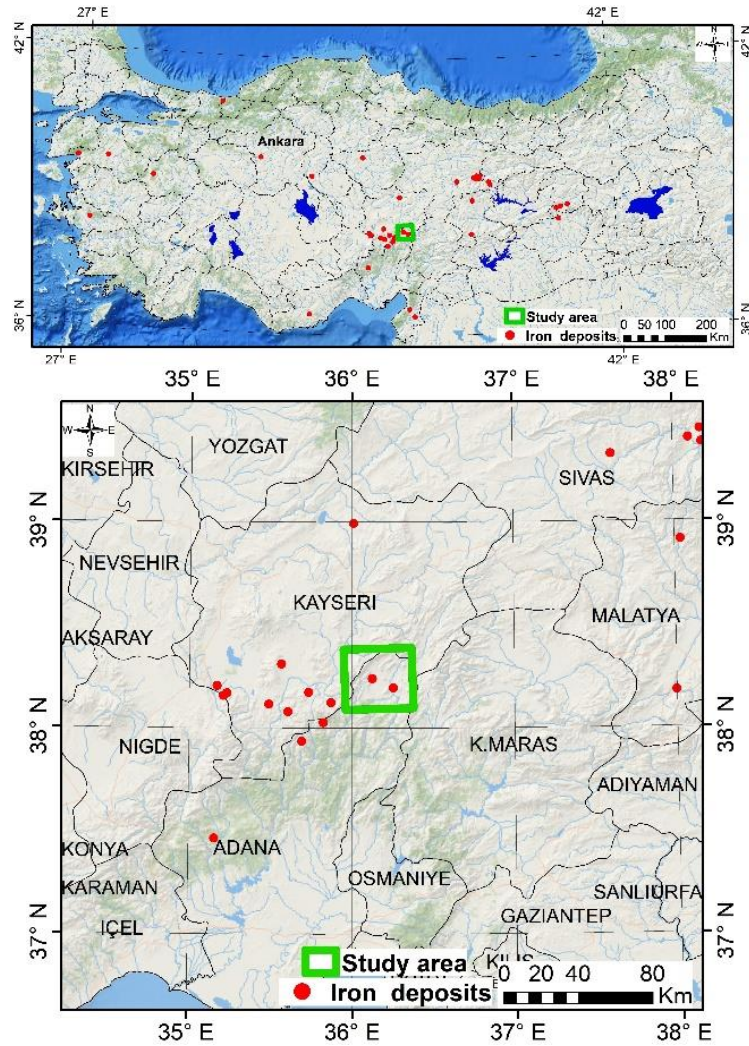
Figure 1: Spatial distribution of iron deposits in Turkey (Tuncel et al., 2017) and location of the study area.

Different image processing techniques such as Band Ratio (BR) and Feature Oriented Principal Component Selection (FOPCS) derived from multispectral Aster and Landsat 8 OLI data can be used to map iron oxides mapping and also for lithological discrimination (Abrams et al. 1983, Kaufman 1988, Crosta and Moore 1989, 1991, Aydal et al., 2007 and Vural et al., 2016). The aim of this research is to investigate the potential of Aster and Landsat-8 OLI to map iron oxides in the cold semi-arid climate with poor vegetation land cover. In this scope, the BR and FOPCS technics are used to detect the different anomalies of iron minerals. In addition, the new band ratio color composition was used to discriminate the lithological formation containing iron oxide.

Geological Setting
The section of the Taurus belt between the North Anatolian Fault, which borders the Munzur Mountains in the east and the Ecemiş Fault in the west, constitutes the "Eastern Taurus" section (Özgül, 1984). According to this division, the study area and its immediate surroundings in the western part of the Eastern Taurus Mountains are represented by rock assemblages covering various tectonic-stratigraphic units with tectonic contacts

that determine the various types of rocks in terms of their specific and separable stratigraphic characteristics and the rock types they cover (Fig. 2) (Özgul and Kozlu, 2002). The Geyikdağ unit includes carbonate and clastic rocks belonging to the Cambrian-Early Tertiary interval.
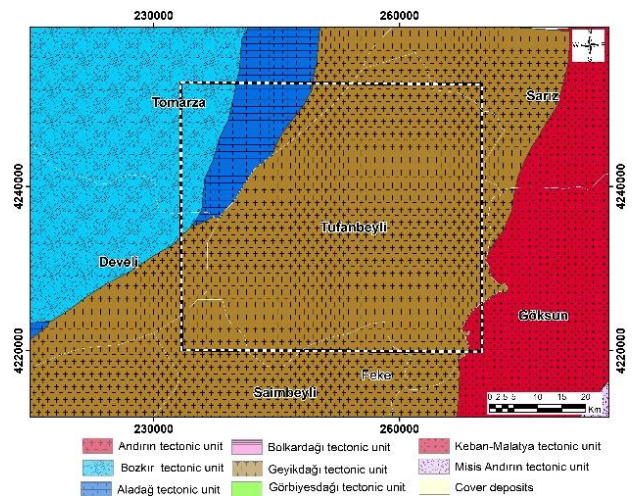

Figure 2. Tectono - stratigraphic units in the western part of the Eastern Taurus maps (Özgül and Kozlu, 2002).

The term 'Unit' is used by Özgül (1971, 1976) for such tectonically related communities, which reflect different basin conditions and each of them is a separate tectono-stratigraphic unit. Apart from the Görbiyesdağı unit, these communities form the continuation of the Geyikdağ, Aladağ and Bozkır units, which were previously defined by in the Middle Taurus Mountains. The Görbiyesdağı unit was first identified and described by Özgül and Kozlu (2002). The steppe unity comprises acidic tuff, basic and ultrabasic rocks and serpentinites with successive sequences representing different facies and environments ranging from continental slope and ocean type rocks deposited in Triassic-Senonian to shelf type rocks. The Aladağ unit includes shelf-type carbonate and clastic rocks representing the Devonian-Cretaceous interval. The Görbiyes unit probably includes the carbonate sequence representing the Jurassic-Late Cretaceous interval and olistolith and olistostromal formations. Görbiyes Dağı unit shows low grade metamorphism. The cover units consist of shallow marine sediments and pelagic sediments (> 1000 m) deposited in the Tertiary-Quaternary interval. There are four major tectono-stratigraphic units in the region: Geyikdağ, Görbiyesdağı, Aladağ and Bozkır tectonic units (Özgül and Kozlu, 2002) (Fig.2).
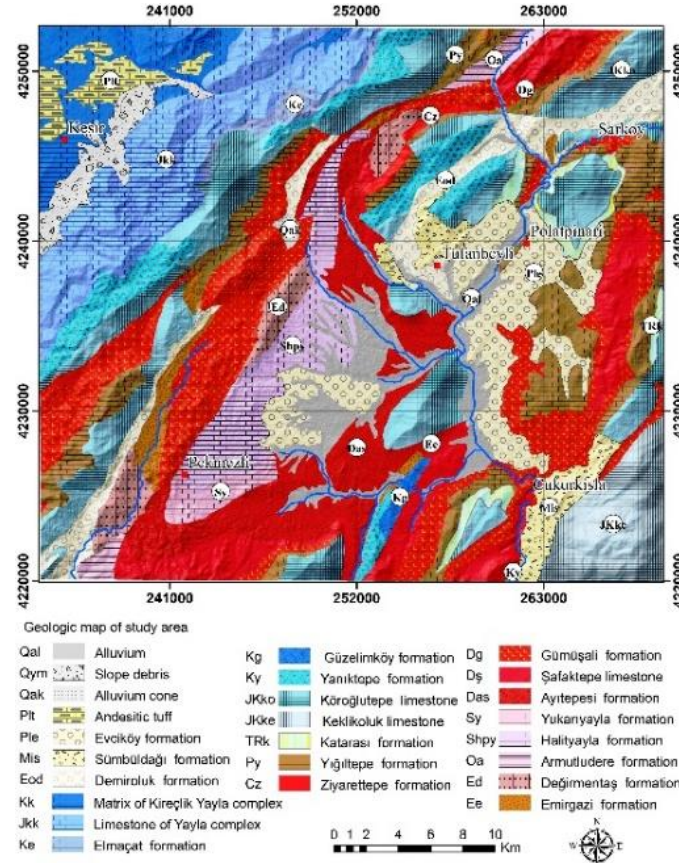

Figure 3: Geological map of study area (Modified from Metin et al., 1990 and Dalkılıç, 2009).

The study area consists of Paleozoic (42.62%), Mesozoic (50.87%) and Cenozoic (6.51%) units (Fig 3). The oldest unit at the basement is the Emirgazi formation of the Geyikdağı unit, characterized by schist, quartzite and metasandstones. Değirmentaş formation conformably overlies the Emirgazi formation. The bottom layers of the unit are represented by clayey limestones and the upper layers are represented by dolomitic limestones. Armutludere and Halityayla formations of Ordovician consist of shale, conglomerate and sandstone in Tufanbeyli autochthonous sequence. Silurian Yukarıyayla formation conformably overlies the Halityayla formation. The Devonian Ayıtepesi formation, which is mainly represented by sandstones, has transitional contact with the Devonian Şafaktepe formation consisting of massive dolomitic limestones. Devonian Gümüşali formation is composed of sandstone, shale, clayey limestones. Carboniferous aged Ziyarettepe and Permian aged Yığıltepe formations are mainly composed of sandstone shale and limestone. The Mesozoic sequence is starting up with the Triassic Katarası formation consisting of crystallized limestone. The Jurassic Cretaceous sequence is followed by Keklikoluk, Köroğlutepe, Yanıktepe, Güzelimköy, Elmaçat and Kireçlikyayla units which are mainly made up of limestones. The Kireçlikyayla ophiolite complex consists mainly of serpentinized dunite, harzburgite, pyroxenite rock assemblages.
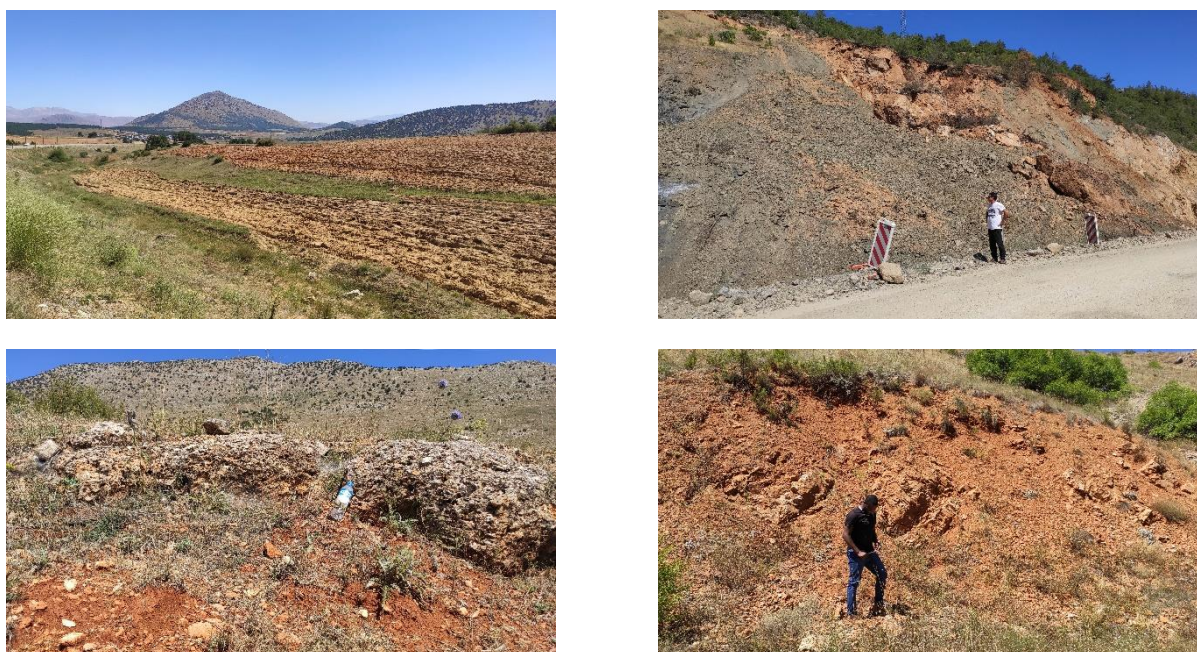
149

Figure 4: Iron oxide deposits observed in the study area.

The Tertiary Demiroluk formation, composing of conglomerate, sandstone and mudstones, unconformably overlies the Mesozoic units. Sümbüldağı and Evciköy formations, which are represented by conglomerates, overlay this unit. Andesitic tuffs constitute the Pliocene cover deposits. Quaternary aged recent and debris deposits are observed around the river valleys and on the flank of the steep slopes, respectively. The presence of iron oxide on Paleozoic and Mesozoic carbonates are well exposed in the study area (Fig 4).

Materials and Methods

Material

Landsat 8 OLI and The Advanced Spaceborne Thermal Emission and Reflection Radiometer (ASTER) images (https://earthexplorer.usgs.gov/), acquired on September 27, 2018 and July 19, 2007 with 0% cloud cover, were used in this study (Table 1).

Method

Radiometric calibration, Atmospheric correction namely "Fast Line-of-sight Atmospheric Analysis of spectral bands/Spectral Hypercubes" (FLAASH) (Envi, 2009; Pour and Hashim 2011); methods were applied to the images in pre-processing stage. As the vegetation cover and iron oxide deposits present similar reflectance spectra, the Normalized Difference Vegetation Index (NDVI), were executed for each image before the main processing stage.

The different extraction information procedures depend on the objectives set, the expected result and especially the types of sensors. Several methods for mineral exploration and geological mapping are usually used in remote sensing data. In the case of this study band ratios and FOPCS are used to discriminate the potential zone of iron oxide. The methodological flowchart applied in this study is shown in Figure 5.
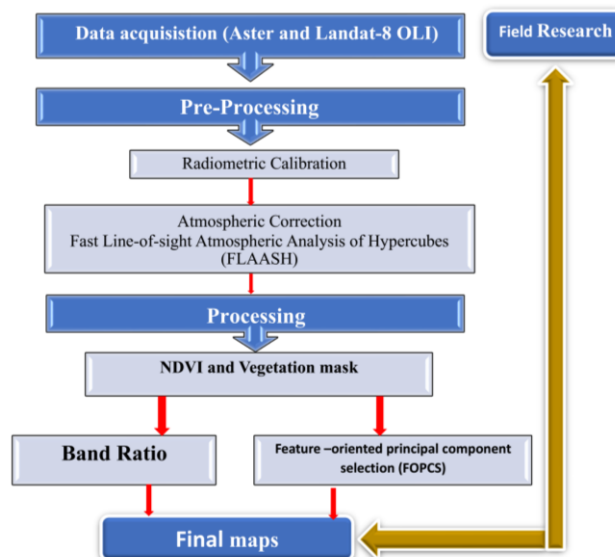
Figure 5: The flow chart of the adopted methodology used in this study.

Table 1: Characteristics of the Aster and Landsat 8 OLI

ASTER

Description	Bands	Wavelength (µm)	Resolution
VNIR	1	0.52-0.60	15 m
	2	0.63-0.69	
	3	0.78-0.86	
	3N	0.78-0.86	
	4	1.60-1.70	
SWIR	5	2.145-2.188	30 m
	6	2.185-2.225	
	7	2.235-2.285	
	8	2.295-2.365	
	9	2.360-2.430	
TIR	10	8.125-8.475	90 m
	11	8.475-8.825	
	12	8.925-9.275	
	13	10.25-10.95	
	14	10.95-11.65	

LANDSAT 8OLI

Description	Bands	Wavelength (μm)	Resolution
Costal	1	0.433-0.453	
	2	0.450-0.515	30 m
Visible	3	0.525-0.60	
	4	0.630-0.680	
NIR	5	0.845-0.885	
SWIR	6	1.560-1.60	30 m
	7	2.100-2.300	
Panchromatic	8	1.360-1.390	15 m
Cirrus	9	0.52-0.90	30 m
TIR	10	10.60-11.19	100 m
	11	11.50-12.51	

Band Ratio

Band Ratio is one of the most methods used in remote sensing for mapping lithological formations and mineral research in recent years. The method consists in dividing the pixel of relectance band by the pixel of the absorption band. The use of band ratio has gained momentum from the research of Sabin (1999). The ratio of two bands removes much of the effect of illumination in the analysis of spectral differences. Table 2 shows the different bands ratios applied in this research.

Feature-oriented principal component selection (FOPCS)

Feature-oriented main component selection (FOPCS) or Crosta Technique is a method based on the Principal component analysis. This method was used for the first time by Crosta and Moore in (1989) and improved by Loughlin (1991). Feature-oriented principal component selection uses only the bands of the image which present a reflection and an absorption. FOPCS is based on the examination of PCA eigenvector loadings to decide which of the principal component images will concentrate the information directly related to the theoretical spectral signatures of specific targets. An important aspect of this approach is that it can predict whether the target surface type is highlighted by dark or light pixels in the corresponding principal component image. Xie et al. (2015) used the Feature Oriented Principal Component Analysis method to extract the information minerals such as limonite, chlorite,

kaolinite, and the alterations in Liaoning Province, based on the analysis of spectral characteristics.

Table 2 List of various band ratio combination using in this study.

Feature	Landsat 8 OLI	Aster	References
	NDVI		
	(5-4) / (5+4)	(3-2) / (3+2)	Rouse and Haas (1973)
	Mineral mapping		
Ferric Iron		2/1	Rowan (1998)
Ferric Oxide		4/3	CSIRO (2003)
Ferrous Iron		5/3 +1/2	Sabin (1999), CSIRO (2003)
Iron oxide	4/2		Sabin (1999)
Ferrous iron	6/5		Sabin (1999)
	Lithological discrimination		
	RGB		
	4/2, 6/5, 6/7		Sabin,1999
		5 /3, 4/6, 6/8	Used in this study

Results and Discussions

NDVI and Masking

Vegetation and iron oxides and have similar reflectance spectra in the wavelength regions covered by Landsat TM bands 1 (blue) and Band 2 (green) equivalent to band 2 (blue) and band 3 (green) in Landsat 8 OLI. These bands are not very favorable for distinguishing iron oxides in areas with high or low vegetation cover. That's why, we have chosen to mask out the vegetation in this study. The NDVI algorithm was used in this research to mask vegetation cover. The NDVI value vary between (-1 and +1). The negative values represent water and snow, and values near zero represent rock and bare soil. The result of the NDVI indicate that the vegetations appear in green color and open area in white color. The vegetation mask at Aster image is denser than Landsat 8 OLI image. This difference is due to the date of acquisition of these images (fig. 6).
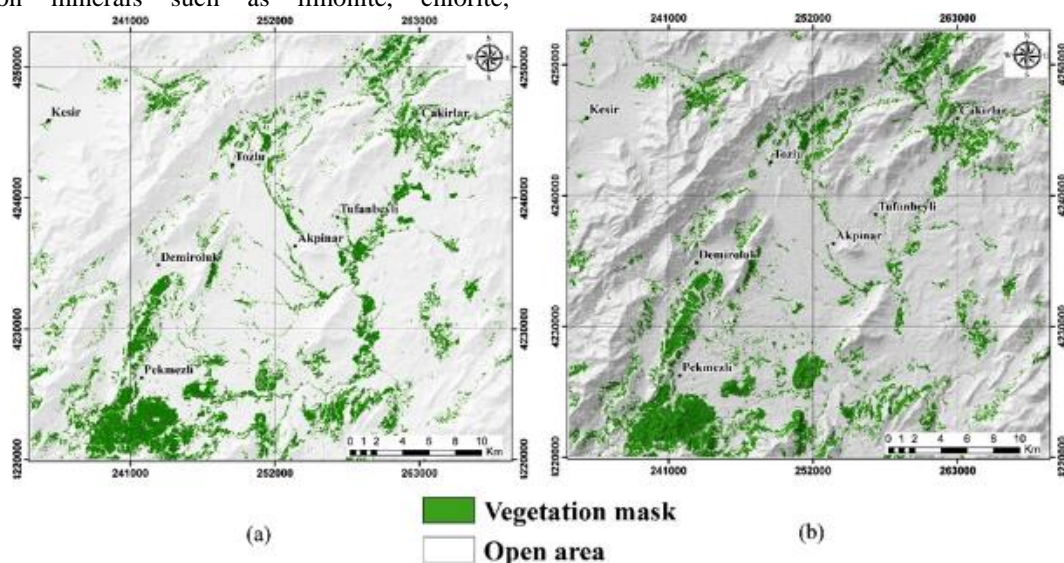

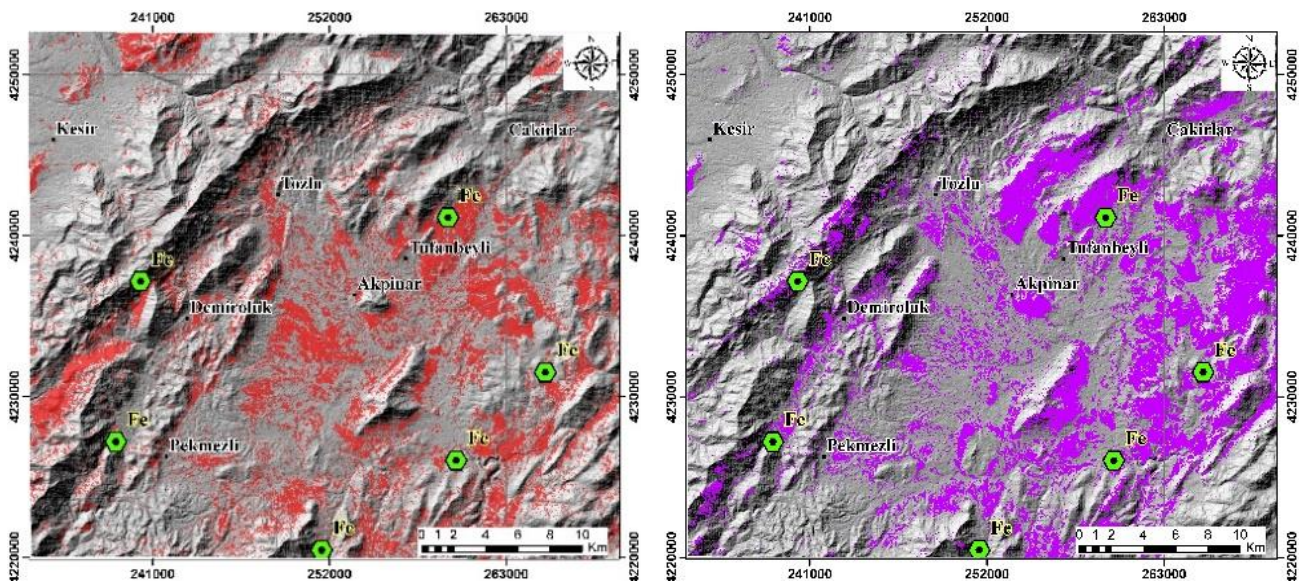Figure 6: Vegetation masking Aster (a), Landsat-8 (b).

Figure 7: Band ratio for iron oxide (4/2) (a), and ferrous (6/5) (b) of Landsat image.

Table 3 Descriptive statistics derived from histogram of Landsat 8 and Aster BR.

	BR	Mean	Std. Dev.	Threshold	Conf. (%)
Aster	Ferric Iron	142	65	207	92%
	Ferric Oxide	128	67	195	92%
	Ferrous Iron	124	64	188	92%
Landsat 8OLI	Iron oxide	161	64	225	92%
	Ferrous Iron	125	73	198	92%

Band Ratio

Many bands ratios used by the previous researches were applied in this study to detect some zone contain the anomalies iron ore deposits. The band ratios 6/5 of ferrous iron and 4/2 of iron oxide for the Landsat image 8 equivalent of 5/4 and 3/1 used by Sabin (1999) and SCIRO (2003) are used. The bands ratios of Ferric iron (2/1), ferric oxide (4/3) and ferrous iron (5/4 +1/2) of the Aster image used by (Sabin, 1999, CSIRO 2003) were applied. The result shows that iron oxide and ferrous iron presents the good anomaly of the Landsat 8 image (Fig. 7 and Table 3). On the other hand, Ferric, ferrous iron and ferric oxide shows a very good anomaly for Aster data (Fig.8 and Table 3).
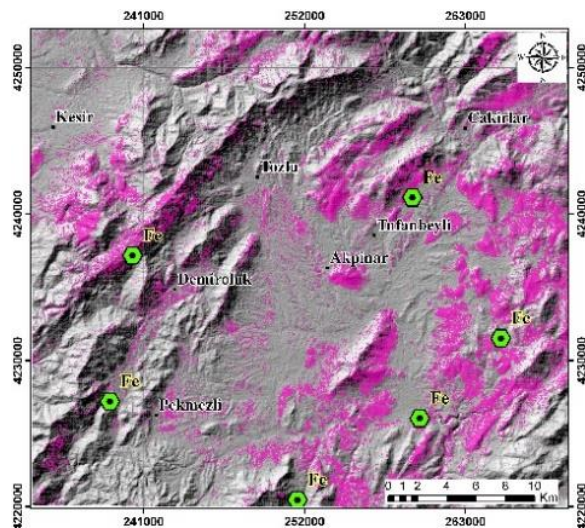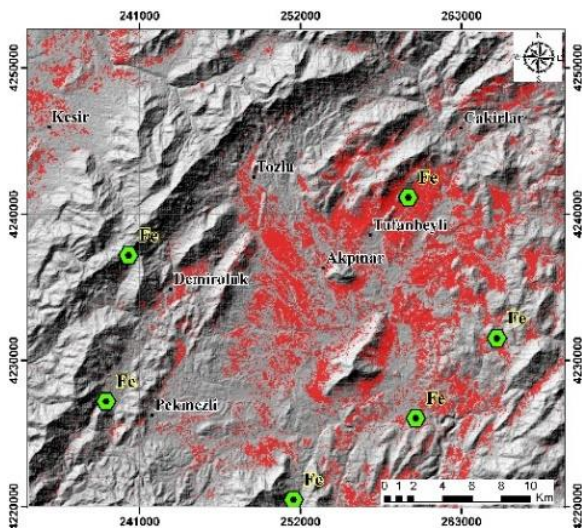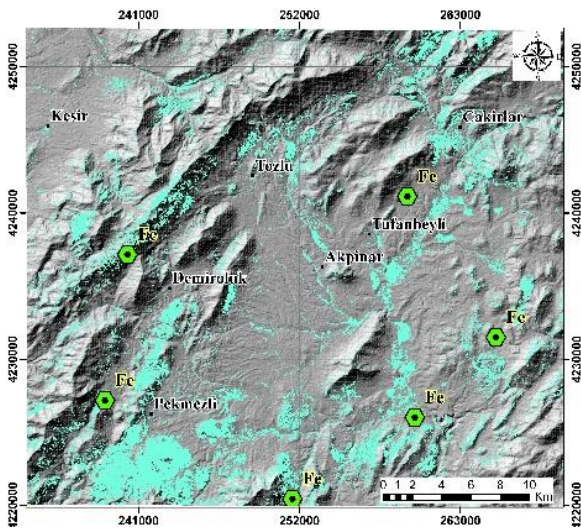
Figure 8: Anomalies of Ferric iron (1/2) (a), Ferric oxide (4/3) (b) and Ferrous iron (5/3+ ½) (c) for Aster in study area.

Feature-Oriented Principal Component Selection (Fopcs)

The bands 2, 4, 5, and 7 of the Landsat 8 image and bands 1, 2, 3, and 4 of the equivalent Aster images of bands 1,3,4 and 7 in Loughlin (1991) Landsat TM to detect anomalies in iron oxide were used. The selection of these bands were based on the iron oxide spectral signature on TM 1 and 3 bands after Loughlin (1991). For the selected bands of the Landsat 8 image, the table presents the statistical summary of bands 2, 4, 5 and 7

for the loading of Eigenvector. Based on this table, PC4 shows the strong values of the opposing signs between bands 2 (0.810) and band 4 (-0.577). For bands 1, 2, 3 and 4 of Aster image, the statistical summary is on the table 4, PC3 and PC4 have opposing signs. In the case of our research we only counted PC4 between band 1 (-0.749) and band 2 (0.661). Because PC4 shows values of opposite signs stronger than PC3. In summary the PC4 has been selected for iron oxide mapping on both Landsat 8 and Aster (Fig. 9 and Table 4).
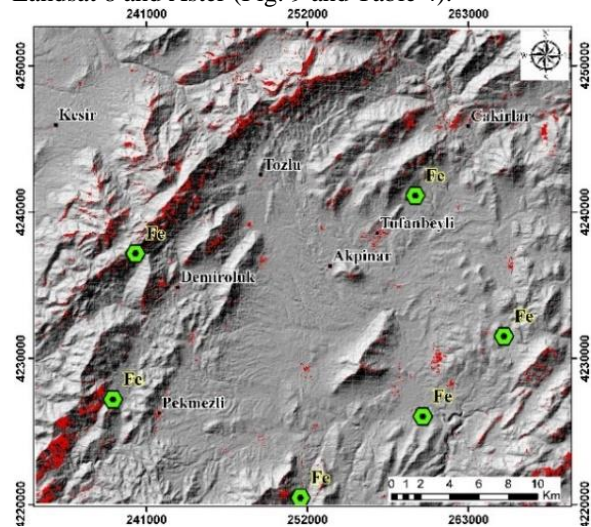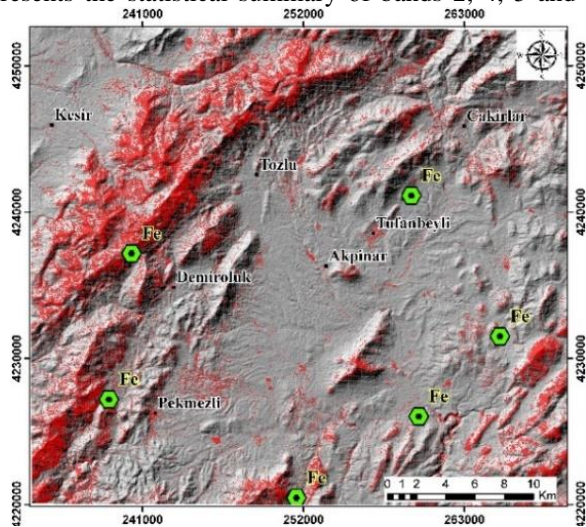
Figure 9: Anomalies of iron in PC4 from Aster (a) and Landsat-8 (b) display in red color.

Table 4: Covariance eigenvector values of the FOPCS for the selected bands (1, 2, 3, and 4) and bands (2, 4, 5 and 7) of ASTER and Landsat 8 OLI respectively.

Aster Masking				
Eigenvector	**Band1**	**Band2**	**Band 3**	**Band4**
PC1	0.136	0.169	0.204	0.954
PC2	0.513	0.603	0.534	-0.294
PC3	-0.395	-0.411	0.8197	-0.045
PC4	-0.749	0.661	-0.029	-0.004
Landsat8 OLI Masking				
Eigenvector	**Band2**	**Band4**	**Band 5**	**Band7**
PC1	0.222	0.448	0.617	0.606
PC2	0.252	0.337	-0.783	0.456
PC3	0.478	0.592	0.032	-0.647
PC4	0.810	-0.577	0.055	0.074

Figure 10: Band ratio (5/3, 4/3 and 6/8) for Aster (a), (4/2, 6/5, 6/7) for Landsat-8 OLI (b) images in RGB and spatial distribution of carbonate units(c).

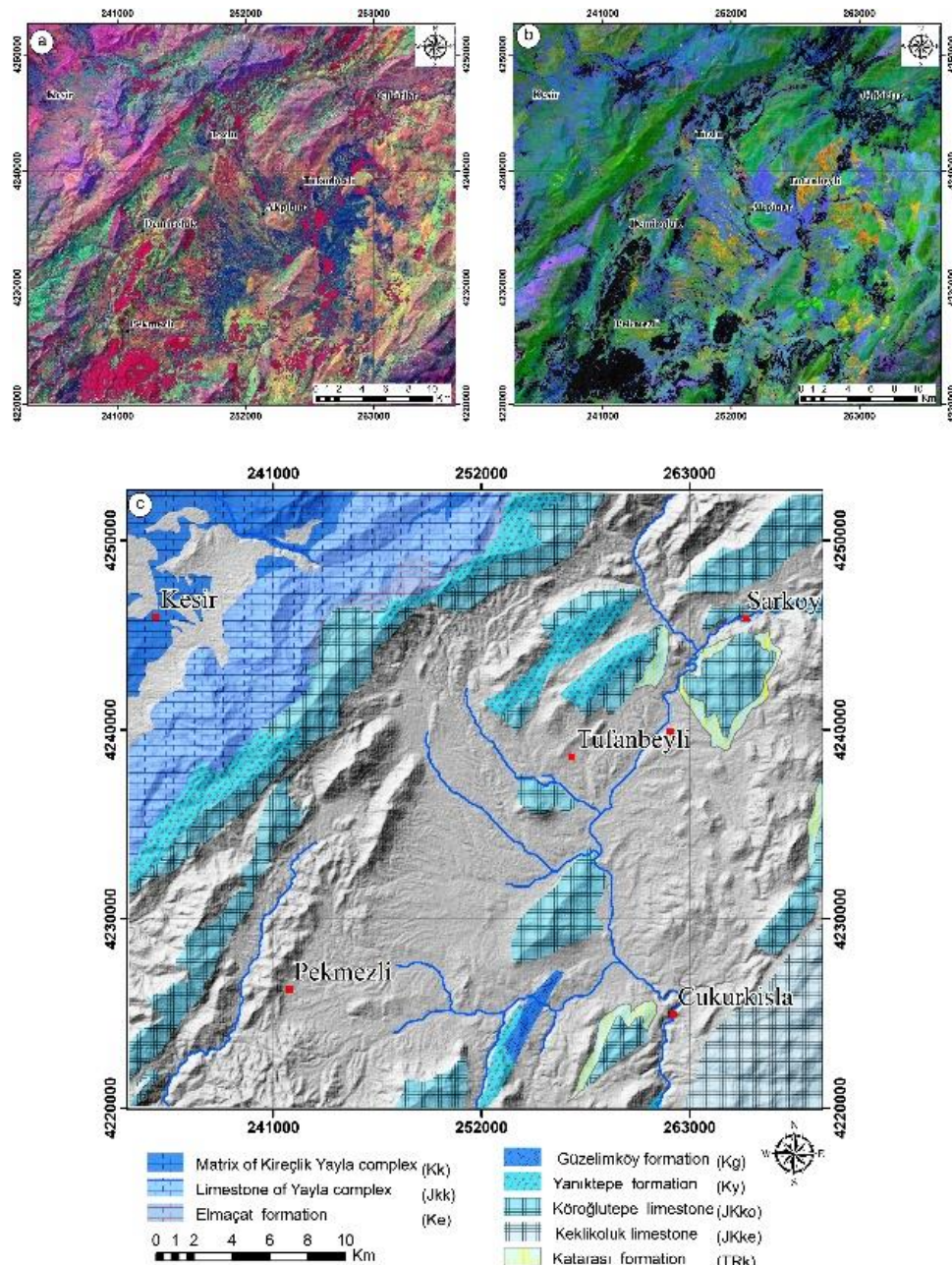The Aster ratio bands (5/3, 4/3 and 6/8) used in this study and the band ratio of Sabin (1999) (4/2, 6/5 and 6/7) of landsat-8 OLI were also applied in this research to discriminate the geological formation contains iron oxide. The selection of these bands is based on the spectral signature of the different minerals or rocks found in our study area. These band rations are displayed in RGB (Fig.10 a,b). According to some research, Anatolide - Tauride iron minerals are contained in limestone carbonate rocks for example. Through to this result, we have found that the iron oxides map in this research are actually on the carbonate rocks (Fig.10c). The results obtained in this research allowed us to make a comparative study not only between the methods but also between the different qualities of data used. A comparative study shows that the significant lithologic groups Carbonate (limestone) such as can Yanıktepe formation, Körüğlutepe formation be extracted well from

ASTER data however, the Değementaş formation and alluvium are mapped well in the Landsat -8 OLI image using BRCC. We found that with both methods applied, the results from aster image present a sharper accuracy and correlation between existing iron oxide data than that of landsat-8 OLI. This small difference is due to the number of bands and the wavelength between these two data. The Aster image presents sharper results than the Landsat-8 OLI because of its number of bands, which is more numerous than that of Landsat. However, Landsat image can cover a wider area (185 km2) than Aster image (60km2).

Conclusion
The objective of this study is to evaluate the potential of Aster and of Landsat-8 OLI data for mapping iron ores deposits in Eastern Taurus, with selected BR and FOPCS methods. After masking the vegetation cover using

NDVI index, the iron ore deposits have been successfully detected using BR and FOPCS methods on Aster and landsat-8 OLI. Together with the verifications made in the field, we confirmed that the accuracy of FOPCS is better than BR methods. The new band ratio color composite (5/3, 4/3 and 6/8) in RGB of Aster image performed in this research showed their efficiency to define the lithological area contains iron oxide than band ratio of Sabin (1999) applied on Landsat-8 OLI data. The majority of iron oxide deposits of the area were hosted by carbonate formations.

In general, the best methods for evaluation of the areas contains mineralization are band ratio, But in this research, LS-Fit present also a good result in visual interpretation. We conclude that, the new zone of iron ore deposits has been found in study area, so it is important to say the BR and FOPCS methods are quite efficient to delineate iron oxide using Aster and Landsat-8 OLI images in cold semi-arid region with poor vegetation cover.

Acknowledgements

References

Abrams, M.J., Rothery, D.A., Pontual, A., (1988). Mapping in the oman ophiolite using enhanced landsat thematic mapper images. *Tectonophysics* 151, 387–401.

Amara, B.N., Aissa, D.E., Maouche, S., Braham, M., Machane, D., Guessoum, N. (2019). Hydrothermal alteration mapping and structural features in the Guelma basin (Northeastern Algeria): contribution of Landsat-8 data. *Arabian Journal of Geosciences,* 12(3), 94.

Arda, N., Tiringa, D., Ateşçi, B., Akça, A., Tufan, E., (2008). Yahyalı (Kayseri)-Mansurlu (Feke-Adana) yöresi demir sahaları maden jeolojisi ara raporu. [Mining geology interim report of Yahyalı (Kayseri)-Mansurlu (Feke-Adana) region iron deposits]. *General Directorate of Mineral Research and Exploration Report No: 44437.* (in Turkish, unpublished).

Avşar, E.O., Bozkurtoğlu, E., Aydar, U., Şeker, D.Z., Kaya, Ş., Gazioğlu, C. (2016). Determining roughness angle of limestone using optical laser scanner. *Internatonal Journal of Environment and Geoinformatics (IJEGEO),* 3(3), 57-75.

Aydal, D., Arda, E., Dumanlilar, Ö., (2007). Application of the Crosta technique for alteration mapping of granitoidic rocks using ETM+ data: case study from eastern Tauride belt (SE Turkey). *International Journal of Remote Sensing,* DOI: 28.3895-3913.0.1080/01431160601105926.

Chen, Z., Christopher, D., Elvidge, David, P, G., (1998). "Vegetation Change Detection Using High Spectral Resolution Vegetation Indices," Remote Sensing Change Detection: *Environmental Monitoring Methods and Applications*, R. S. Lunetta and C. D. Elvidge (Eds.), 181–190. Ann Arbor Press, Chelsea, Michigan.

Cihnioğlu, M., Isbasarir, O., Ceyhan, U., Adigüzel O., (1994). *Demir Envanteri. [Iron inventory of Turkey].* General Directorate of Mineral Research and Exploration 367 p. (in Turkish, unpublished).

Crosta, A., Moore, J., (1989). Geological mapping using Landsat Thematic Mapper imagery in Almeria Province, south-east Spain. *International Journal of Remote Sensing.* DOI. 10.1080/01431168908903888.

CSIRO.,2003.http://www.syd.dem.csiro.au/research/MMTG/Exploration/ASTER/ASTER.htm.

Dalkılıç, H., (2009). *1/100:000 Ölçekli Jeoloji Haritaları Serisi Kayseri L-35 Paftası* Jeoloji Etütkleri Dairesi No:233 S.39 Maden Tetkik Ve Arama Genel Müdürlüğü, Ankara-Türkiye (InTurkish).

Dayan, S., (2007). *Adana-Mansurlu Attepe civarındaki demir yataklarının jeolojik, petrografi ve yapısal özelliklerinin incelenmesi.* [Geological, petrographic and structural investigation of iron deposits in the region of Mansurlu, Attepe-Adana]. Master Thesis, Ankara University 125 p, Ankara (In Turkish, unpublished).

Dayan, S., Ünlü, T., Sayılı, I., (2008). Adana-Mansurlu Attepe Demir Yatağı'nın maden jeolojisi. [Mining geology of Attepe Iron Deposit, Mansurlu-Adana]. *J Geol Eng* 32(2):1–44 (in Turkish with English abstract).

Ducart, D. F., Silva, A. M., Toledo, C. L. B., Assis, L. MD. (2016). Mapping iron oxides with Landsat-8/OLI and EO-1/Hyperion imagery from the Serra Norte iron deposits in the Carajás Mineral Province, Brazil. *Brazilian Journal of Geology*, 46(3), 331-349.

ENVI, (2009). *Atmospheric Correction Module: QUAC and FLAASH* User's Guide.

Gad, S., Kusky, T. (2007). ASTER spectral ratioing for lithological mapping in the Arabian–Nubian shield, the Neoproterozoic Wadi Kid area, Sinai, *Egypt. Gondwana Research, 11*(3), 326-335.

Gazioğlu, C., Alpar, B., Yücel, ZY., Müftüoğlu, AE., Güneysu, C., Ertek, TA. (2014). Morphologic Features of Kapıdağ Peninsula and its Coasts (NW-Turkey) using by Remote Sensing and DTM. *International Journal of Environment and Geoinformatics (IJEGEO)* 1(1), 48-63. DOI: 10.30897/ijegeo.300739

Huang, S., Chen, S. B., Zhang, YZ. (2018). Comparison of altered mineral information extracted from ETM+, ASTER and Hyperion data in Águas Claras iron ore, Brazil. *IET Image Processing,* 13(2), 355-364.

İncekara, A., Seker, D. Z., Tezcan, C. S., Bozkutoglu, E., Gazioglu, C. (2017). Interpreting temperaturebased discontinuity and roughness of rock surfaces by using photogrammetric technique. *International Journal of Environment and Geoinformatics (IJEGEO),*4(3), 206–213. DOI: 10.30897/ijegeo.348806.

Küçük Matçı, D., Avdan, U. (2019). Optimization of Remote Sensing Image Attributes to Improve Classification Accuracy, *International Journal of Environment and Geoinformatics (IJEGEO),* 6(1): 50-56. DOI: 10.30897/ijegeo.466985.

Lillesand, T. M., Kiefer, R., M., Chipman J., W., (2004). *Remote Sensing and Image Interpretation, fifth edition.* John Wiley & Sons, Inc., New York, New York, 2004.

Loughlin, W.P., (1991). Principal component analysis for alteration mapping. *Photogrammetric Engineering and Remote Sensing,* 57(9), 1163-1169.

Mars, J.C., Rowan, L.C., (2006). Regional mapping of phyllic- and argillic-altered rocks in the Zagros magmatic arc, Iran, using Advanced Spaceborne Thermal Emission and Reflection Radiometer (ASTER) data and logical operator algorithms. *Geosphere* 2, 161 –186.

Metin, S., Ayhan, A., Papak, I., (1990). *1/100:000 Ölçekli Jeoloji Haritaları Serisi Elbistan L-36 Paftası* Jeoloji Etütkleri Dairesi No:233 S.20 Maden Tetkik Ve Arama Genel Müdürlüğü, Ankara-Türkiye (InTurkish).

Özgül, N., (1984), Stratigraphy and tectonic evolutionof the central Taurides; Geology of the Taurides, *Interna.Symp.,* 77-90, Ankara.

Özgül, N., Kozlu, H., (2002). Kozan-Feke (Doğu Toroslar) Yöresinin Stratigrafisi ve Yapısal Konumu ile İlgili Bulgular, *Türkiye Petrol Jeologları Derneği Bülteni,* Sayı 14, No: 1, s. 1-36.

Pour, A.B., Park, Y., Park, T.Y. S., Hong, J. K., Hashim, M., Woo, J., Ayoobi, İ., (2019). Evaluation of ICA and CEM algorithms with Landsat-8/ASTER data for geological mapping in inaccessible regions, *Geocarto International,* 34:7, 785-816, DOI: 10.1080/10106049.2018.1434684

Pour, A.B., and Hashim, M., (2011). Spectral transformation of ASTER data and the discrimination of hydrothermal alteration minerals in a semi-arid region, SE Iran. *International Journal of the Physical Sciences,* 6(8), 2037–2059.

Rajendran, S., Thirunavukkarasu, A., Balamurugan, G., Shankar, K., (2011). Discrimination of iron ore deposits of granulite terrain of Southern Peninsular India using ASTER data. *Journal of Asian Earth Sciences* 41, 99–106.

Sabins, F.F., (1999). Remote sensing for mineral exploration. *Ore geology reviews*, 14(3-4), 157-183.

Safari, M., Maghsoudi, A,. Pour, A,B., (2018). Application of Landsat-8 and ASTER satellite remote sensing data for porphyry copper exploration: a case study from Shahr-e-Babak, Kerman, south of Iran. *Geocarto international*, 33(11), 1186-1201.

Sengupta, A., Adhikari, M. D., Maiti, S., Maiti, S. K., Mahanta, P., Bhaumick, S., (2019). Identification and mapping of high-potential iron ore alteration zone across Joda, Odisha using ASTER and EO-1 hyperion data. *Journal of Spatial Science,* 64(3), 491-514.

Shirazi, A., Hezarkhani, A., Shirazy, A., (2018). Remote Sensing Studies for Mapping of Iron Oxide Regions, South of Kerman, IRAN. *International Journal of Science and Engineering Applications* 7(4), 45-51 ISSN-2319–7560.

Tiringa, D., Çelik, Y., Ateşçi, B., Akça, I., Keskin, S., (2011). *Kayseri-Adana Havzası demir aramaları ve Menteş Dere (Yahyalı-Kayseri) ruhsat sahasının maden jeolojisi raporu.* [Mining geology report of iron explorations in Kayseri-Adana Basin and Menteş Dere (Yahyalı-Kayseri) license area]. Mineral Research and Exploration Report No: 11435. (in Turkish, unpublished).

Tuncel, S., Ari, N., Yoleri, B., Şahiner, M., (2017). *Dünyada ve Türkiye'de Demir.* Maden Tetkik ve Arama Genel Müdürlüğü Fizibilite Etütleri Daire Başkanlığı. S.1- 25.

Ünlü, T., Dumanlılar, Ö., Tosun, L., Akıska, S., Tiringa, D., (2019). Chapter 5 Turkish Iron Deposits. Springer Nature Switzerland AG 2019. Mineral Resources of Turkey, *Modern Approaches in Solid Earth Sciences* 16, DOI: 10.1007/978-3-030-02950-0_5.

Vural, A., Corumluoglu, O., Asri, I. (2016). Exploring Gördes Zeolite Sites by Feature Oriented Principle Component Analysis of LANDSAT Images. Caspian *Journal of Environmental Sciences,* 14(4), 285-298.

Xie, M.H., Zhang, Q., Chen, S.B., (2015). Extraction of alteration anomaly information by feature-based principal component analysis from ASTER data. Earth Science *Journal of China University of Geosciences* 40, 1381e1385 (in Chinese with English abstract).

Zoheir, B., El-Wahed, M, A., Pour, A,B., Abdelnasser, A., (2019). Orogenic Gold in Transpression and Transtension Zones: Field and Remote Sensing Studies of the Barramiya–Mueilha Sector, Egypt. *Remote Sens.* 11, 2122; DOI: 10.3390/rs11182122.